Real-Time Observation of the Spin-State Mixing Process of a Micellized Radical Pair in Weak Magnetic Fields by Nanosecond Fast Field Switching

Tomoaki Miura[†] and Hisao Murai*[,‡]

Graduate School of Science and Engineering and Department of Chemistry, Faculty of Science, Shizuoka University, 836 Oya, Surugaku, Shizuoka 422-8529, Japan

Received: September 18, 2007; In Final Form: December 1, 2007

The singlet−triplet spin-state mixing process of a singlet-born radical pair confined in a sodium dodecyl sulfate (SDS) micelle was studied by observing the nanosecond switched external magnetic field (SEMF) effect on the transient absorption signals. A long-lived singlet radical pair is generated by the photoinduced bond cleavage reaction of tetraphenylhydrazine in an SDS micelle. Application of off−on type SEMF results in the increase of the free radical yield contrary to the decrease produced by an applied static magnetic field. The S−T mixing process in low magnetic field was observed by means of a delay-shift SEMF experiment. Observed incoherent mixing processes are explained in terms of the interplay between coherent hyperfine interaction and fast dephasing processes caused by the fluctuation of electron-spin interactions. Singlet−triplet and triplet−triplet dephasing rate constants are determined independently to be 2×10^8 and 0.2×10^8 s^{-1}, respectively, by a simulation based on a modified single-site Liouville equation. This is the first direct observation of the incoherent spin-state mixing process at magnetic fields comparable to the hyperfine interactions of the radical pair.

Introduction

Effects of magnetic fields on chemical and biochemical reactions have been attracting much interest over the last 30 years. The magnetic field effect (MFE) based on the radical-pair mechanism is the most commonly known in chemical reactions where the generation of radical pairs or radical-ion pairs is involved.[1] The magnetic-field-dependent mixing process between singlet and triplet states of radical pairs is a key process with respect to yielding reaction products of the radical pair, because the recombination reaction is generally spin-state-selective. The spin-state mixing process is governed by the coherent hyperfine interaction (HFI) at weak magnetic fields of less than 10 mT. In particular, the so-called low-field effect[2−4] whose sign is opposite to the ordinary MFE is peculiar and has received a lot of attention in the context of the possible mechanism of bird navigation in the earth's magnetic field.[5,6] One of the possible candidates for the parent molecule of the radical pair responsible for birds' magnetic field sensing is cryptochrome, which is one of the flavoproteins. According to recent reports, a long-lived radical pair is generated by the photoirradiation of the protein.[7,8] In such inhomogeneous biological systems, diffusion dynamics of the radical pairs is considered to be restricted by interactions with, for example, protein pockets or surfaces.[9,10] In some cases, the restricted motion of the radical pair results in extension of the lifetime.

However, most experiments and theoretical work concerning low-field spin dynamics are performed in the systems of a short-lived radical pair in homogeneous solution, in which the lifetime of the radical pair is so short that the coherent spin dynamics is the only factor that determines the magnetic field dependence of the reaction yield (MARY).[11,12] From the biological point of view, spin dynamics of long-lived radical pairs confined in inhomogeneous environments are of much interest.

A novel insight into the spin-state mixing process in low magnetic fields, explained in terms of the interplay between HFI and fast dephasing processes, has been obtained from a detailed analysis of the dynamic shift to high field (broadening) of time-resolved and nanosecond pulsed MARY spectra in the system of a long-lived triplet radical pair in an SDS micelle.[13,14] The dephasing processes are considered to be induced by the fluctuation of inter-electron-spin interactions such as the exchange interaction (J) and/or dipole−dipole interaction (D) caused by the diffusive motion of the radical pair in the micellar supercage.[15−17]

Accordingly, it is clear that the low-field spin dynamics are strongly coupled with the molecular dynamics of the long-lived radical pair. There are many possibilities for probing the molecular dynamics of radical pairs confined in inhomogeneous environments by analyzing the low-field spin dynamics of the radical pairs. A real-time observation of the spin-state mixing process in low magnetic field is necessary to clarify the problem.

In the present work, we demonstrate the first real-time observation of the spin-state mixing process of a photolytically generated, singlet-born, micellized radical pair by means of a transient absorption-detected nanosecond switched external magnetic field (SEMF) method. From the theoretical analysis of the experimental time evolution, we discuss the dephasing processes in detail in the context of molecular motion and interspin interactions of the long-lived radical pair.

Experimental Section

Tetraphenylhydrazine [$(C_6H_5)_2N-N(C_6H_5)_2$, TPH] was synthesized by oxidization of diphenylamine by potassium permanganate as reported previously[18] and recrystallized from

* To whom correspondence should be addressed. Tel and Fax: +81-54-238-4753. E-mail: shmurai@ipc.shizuoka.ac.jp.
[†] Graduate School of Science and Engineering.
[‡] Department of Chemistry, Faculty of Science.

10.1021/jp077505x CCC: $40.75
Published on Web 02/29/2008

benzene. Sodium dodecyl sulfate (SDS) was used as received. All of the reagents were supplied by Wako Co. Ltd. The sample solution was prepared by first dissolving TPH in a small amount of benzene, and the benzene solution was added to an aqueous solution of SDS. The total concentrations of TPH, SDS, and benzene were 0.1, 100, and 100 mM, respectively. The sample solution was deoxygenated by bubbling nitrogen gas before and during measurement.

The experimental setup of transient absorption-detected nanosecond SEMF measurement is essentially the same as that reported elsewhere except for a few points.[4,13,14] A XeCl excimer laser (Lambda Physik COMPex, full width at half-maximum (fwhm) of ca. 17 ns and wavelength of 308 nm) and continuous-wave Xe arc lamp were used as pump and probe light sources, respectively. The sample solution was transferred to the sample cell, where a photochemical reaction takes place, without recycling. The transient absorption signal at $\lambda = 690$ nm, which was assigned to a diphenylaminyl ($(C_6H_5)_2N^{\bullet}$, DPA) radical,[19] was monitored for the observation of static and switched MFEs.

The nanosecond magnetic field pulser described in the previous reports[13,20] was used for SEMF experiments. The rise and fall times of the magnetic field were both ca. 15 ns. The maximum amplitude and duration of the pulsed field were ca. 30 mT and 1 μs, respectively.

Theory

We have carried out theoretical simulations based on a modified single-site Liouville equation, in which HFIs are evaluated by a semiclassical approach.[21] The method of simulation is intrinsically identical with that described in ref 13 except for minor changes. A semiclassical approximation of HFI causes serious problems on simulations in much lower magnetic fields than HFI. However, we are interested in the spin dynamics at fields comparable to or larger than HFI. Thus, this approximation causes few problems in our case. The time evolution of the density ket, which is initially a pure singlet state, is calculated by numerical solution of the Liouville equation

$$\mathrm{d}|\rho(t)\rangle/\mathrm{d}t = -(iH^{\times} + \hat{W} + \hat{R})|\rho(t)\rangle \qquad (1)$$

where $H^{\times}$, $\hat{W}$, and $\hat{R}$ represent the commutator of the spin Hamiltonian, the superoperator of chemical reaction, and the relaxation operator including dephasing terms, respectively.

The Zeeman interaction and semiclassical HFI are involved in the spin Hamiltonian; J and D are not involved directly because of the frequent fluctuation of these interactions. The effect of SEMF is taken into account approximately by gradually changing B_0 of the Zeeman term in each time step. The rise of SEMF is evaluated by a single-exponential function with a time constant of 15 ns. The norm and direction of the semiclassical nuclear vector in terms of HFI are evaluated by a statistical random sampling method.

With respect to $\hat{W}$, the generation kinetics of the radical pair, recombination via a singlet state, and escape from the micellar cage are accounted for as chemical reactions. Photocleavage of TPH is so fast that the shape of the laser pulse determines generation of the radical pair.[22] The time profile of the laser pulse is evaluated by a Gaussian function with fwhm of 17 ns. Other rate constants are taken from reported values obtained by pulsed RYDMR experiments, which are $k_{rec} = 5 \times 10^6\ s^{-1}$ and $k_{esc} = 3.5 \times 10^5\ s^{-1}$ for the recombination rate and escape rate, respectively.[19]

The relaxation operator $\hat{R}$ is roughly divided into two terms, which are the conventional spin relaxations of each radical and spin dephasing processes ($R_{dephasing}$) characteristic of the radical pairs. The intraradical relaxations, T_1 and T_2, of each DPA radical are calculated by the high-field approximation as

$$\frac{1}{T_1} = \frac{\tau_c}{6}\frac{[A{:}A]}{1+\omega_e^2\tau_c^2} \quad \text{and} \quad \frac{1}{T_2} = \frac{1}{2T_1}\frac{\tau_c[A{:}A]}{12} \qquad (2)$$

where $[A{:}A] = \sum_{x,y,z}(a_i - a_{iso})^2$ is the anisotropic term of the HFI and τ_c is the rotational correlation time.[23] The high-field approximation is not applicable at weak fields comparable to HFI to be exact. However, intraradical relaxations are considered to be slower than both the dephasing process stated below and the dephasing-assisted incoherent mixing process explained in the following sections. Thus, the high-field approximation used here does not cause a severe problem for simulations.

The dephasing terms of the radical pair involve singlet−triplet dephasing (STD) and triplet−triplet dephasing (TTD) as

$$R_{dephasing} = w_{STD}\sum_{i=-1,0,+1}(|ST_i\rangle\langle ST_i| + |T_iS\rangle\langle T_iS|) + w_{TTD}\sum_{j=+1,-1}(|T_jT_0\rangle\langle T_jT_0| + |T_0T_j\rangle\langle T_0T_j|) \qquad (3)$$

where w_{STD} and w_{TTD} are the rate constants of STD and TTD, respectively. These dephasing processes are considered to be caused by fluctuations of J and/or D.[15,17]

The time profile of the transient absorption signal is represented by the sum of the radical-pair population [$tr\rho(t)$] and the yield of free radicals that have escaped from the micelle as

$$\Delta A(t) \propto tr\rho(t) + \int_0^t k_{esc}\, tr\rho(\tau)\,\mathrm{d}\tau \qquad (4)$$

SCHEME 1: Photoreaction Process of TPH in an SDS Micelle, Where the Bracket Represents the Radical Pair

$$\mathrm{TPH} \xrightarrow{h\nu} {}^1\mathrm{TPH}^* \qquad \text{Photo excitation}$$

$${}^1\mathrm{TPH}^* \xrightarrow{<7\ \mathrm{ps}} {}^1[\mathrm{DPA}\cdot\cdot\mathrm{DPA}] \qquad \text{Bond cleavage}$$

$${}^1[\mathrm{DPA}\cdot\cdot\mathrm{DPA}] \leftrightarrows {}^3[\mathrm{DPA}\cdot\cdot\mathrm{DPA}] \qquad \textbf{Spin state mixing}$$

$${}^1[\mathrm{DPA}\cdot\cdot\mathrm{DPA}] \xrightarrow{k_{rec}} \mathrm{TPH} \qquad \text{Recombination}$$

$${}^{1,3}[\mathrm{DPA}\cdot\cdot\mathrm{DPA}] \xrightarrow{k_{esc}} \text{free DPA radicals} \qquad \text{Escape}$$

Results and Discussion

The photoreaction process of TPH in a SDS aqueous solution reported by Fukuju et al.[24,25] is shown in Scheme 1. The excited singlet state is generated by photoirradiation of TPH. A N−N bond cleavage reaction proceeds within a few picoseconds, giving a radical pair consisting of two identical DPA radicals, which exhibit a transient absorption band around $\lambda = 690$ nm.[19]

(I) Static MFE and Time-Resolved MARY Spectra. The transient absorption time profile at $\lambda = 690$ nm with and without a static external magnetic field of 50 mT is shown in Figure 1. The transient signal of the DPA radical shows a decay component (~1 μs) at early time and a flat component, which is assigned to the escaped free radical, at late time. If k_{esc} is much smaller than k_{rec}, the radical-pair lifetime in 0 mT is determined by a geminate recombination reaction, with a rate 4 times smaller than k_{rec}.[26] The reported rate constants indicate

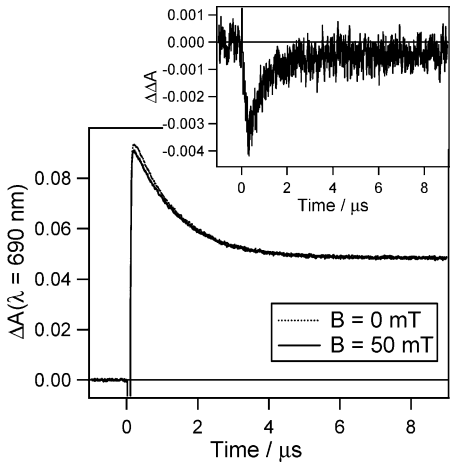

Figure 1. Time profiles of the transient absorption signal of a DPA radical ($\lambda = 690$ nm) with and without a static external magnetic field. The subtracted time profile $\Delta\Delta A = \Delta A(B = 50\ \text{mT}) - \Delta A(B = 0\ \text{mT})$ is shown in the inset.

that the observed decay component reflects the geminate recombination of the singlet radical pair.

By application of a magnetic field, the yield of the DPA radical decreases, as shown in Figure 1 and its inset. The sign of the observed MFE is consistent with the conventional theory of MFE by the radical-pair mechanism, as indicated below.[1] The application of an external magnetic field induces the Zeeman splitting in triplet energy levels of the radical pair; thus, the $S-T_{+1}$ and $S-T_{-1}$ spin-state mixing by HFI is inhibited. Because the radical pair is generated from the singlet state, inhibition of $S-T$ mixing increases the relative yield of singlet radical pairs and thus promotes in-cage recombination.

Generally, observation of MFEs in singlet radical-pair systems is difficult because of a faster recombination reaction of the singlet radical pair than the diffusion and spin-mixing process. In the present case, however, the MFE can be successfully observed because of the low recombination reactivity. The reason for low reactivity is considered to be the conformational change around the N atom and the delocalization of the unpaired electron over two benzene rings in the DPA radical.[27]

The rising component ($\sim$200 ns) of the subtracted time profile at early time reflects the recombination rate, whereas the decaying one, with a much longer time constant, is due to some sort of spin relaxation in the field of 50 mT. The observed MFE is relatively small (4% in 50 mT) compared with triplet micellized radical-pair systems reported previously.[14,26] This is also due to slow recombination reaction kinetics comparable to the spin-relaxation process (including dephasing-assisted spin-state mixing, shown later) between radical-pair sublevels.

Time-resolved MARY spectra obtained by plotting the static MFE on transient absorption signals at each instant of time are shown in Figure 2.[4,13,14] The spectrum at late time ($t = 1\ \mu$s) does not reach a plateau at much higher magnetic field, indicating the contribution of a conventional relaxation (T_1) mechanism mainly due to the anisotropic HFI.[28,29]

On the other hand, the spectrum at 200 ns, which is the earliest limit of our measurement, seems to reach a plateau at relatively low magnetic field. This is because we can exclude the T_1 mechanism by observing the MFE at an earlier time than T_1 operates, usually several hundred nanoseconds or longer. The spectrum is interpreted mainly in terms of the hyperfine mechanism. The effective HFI of the radical pair, which has been believed to be identical with $B_{1/2}$ (magnetic field giving MFE of half of the saturation value), is determined to be $a_{\text{eff}} =$ 3.03 mT from reported hyperfine coupling constants of the DPA radical.[1,30] The spectrum at 200 ns is fitted by assuming a Lorentzian shape function as

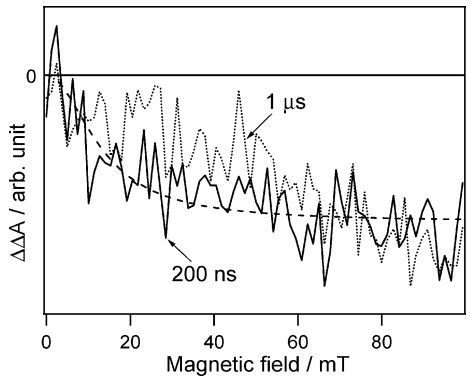

Figure 2. Time-resolved MARY spectra obtained by plotting $\Delta\Delta A$ at 200 ns (solid line) and that at 1 μs (dotted line) as a function of the applied magnetic field. Spectra are normalized to the maximum of $\Delta\Delta A$. The broken line shows curve fitting of the spectrum at 200 ns using a Lorentz function (see text).

$$\Delta\Delta A(B) = \Delta\Delta A_{\text{sat.}} \frac{B^2}{B^2 + {B_{1/2}}^2} \tag{5}$$

where $\Delta\Delta A_{\text{sat.}}$ is the saturation value of $\Delta\Delta A$ at high magnetic field (Figure 2, dashed line). The experimental $B_{1/2}$ value obtained is 13 mT, which is somewhat larger than a_{eff}.

Recently, Rodgers et al.[31] have reported that a_{eff} is approximately equal to $B_{1/2}$ only when the radical-pair lifetime is comparable to the time scale of a_{eff}. It is obvious that the lifetime of the radical pair in our system is much longer than the time scale of a_{eff}, and the rule of $B_{1/2}$ does not hold. However, the $B_{1/2}$ values obtained by their pure quantum-mechanical simulations are smaller than a_{eff} if the radical-pair lifetime is much longer than the time scale of a_{eff}. Consequently, the larger $B_{1/2}$ than a_{eff} at early time is considered to be mainly due to the fast dephasing process characteristic of micellized radical pairs.[14]

In the present system, the short $S-T_0$ dephasing time of 50 ns was previously reported from the analysis of the time-dependent SCRP pattern in X-band time-resolved EPR spectra.[25] This fact also supports the idea that observed MARY spectra are affected by the fast dephasing process. A more detailed analysis is possible by observing much faster spin dynamics using nanosecond SEMF.

(II) Nanosecond SEMF Effect. *(1) SEMF from 0 mT.* We have applied a SEMF of 28 mT at 100 ns after a laser shot in the absence of a static magnetic field. The duration of the pulsed field is 950 ns, which is almost the maximum limit of the SEMF device used here. The time profile obtained by subtracting the transient signal of the DPA radical without magnetic field switching from that with 0−28 mT field switching is shown in Figure 3. Despite noise from the current pulser just after switching on and off, the sign of the subtracted signal during pulse duration is positive. Thus, the radical-pair lifetime and free-radical yield are increased by nanosecond magnetic field switching contrary to the result observed by the applied static field.

This opposite effect is interpreted on the basis of transient control of the energy levels of radical-pair spin states, as shown in Figure 4. The singlet radical pair proceeds to spin mixing with three triplet sublevels equally in the absence of a magnetic field and reaches a steady state of $[S]:[T] = 1:3$ in a few tens of nanoseconds. The application of a switched magnetic field

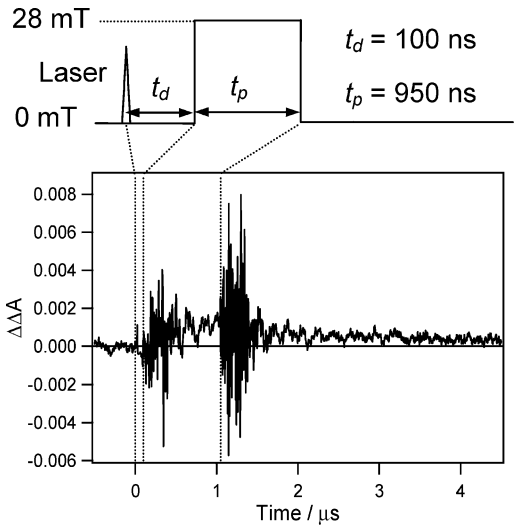

Figure 3. Effect of nanosecond external magnetic field switching from 0 to 28 mT on the time profile of transient absorption. $\Delta\Delta A$ here is defined as $\Delta\Delta A = \Delta A(\text{SEMF}) - \Delta A(0\text{ mT})$. Timing of the field switching (delay time of 100 ns and duration of 950 ns) is indicated by the chart attached above the experimental data.

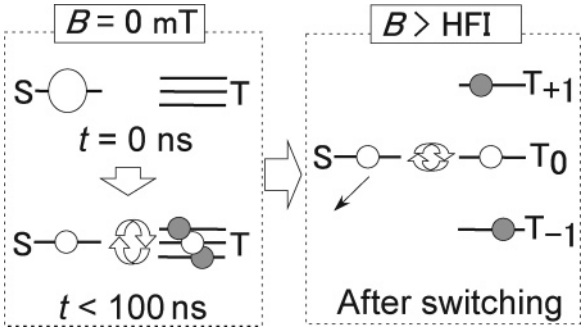

Figure 4. Mechanism of the nanosecond SEMF effect on the singlet-born radical pair. Population of the radical pair is expressed by the size of the circle. Gray-colored circles represent the radical-pair populations in the $T_{\pm1}$ states before and immediately after the field switching.

instantaneously splits the Zeeman energies of triplet sublevels; namely, the radical pairs populated in T_{+1} and T_{-1} states (colored gray in Figure 4) are energetically isolated. Because the switched field of 28 mT is sufficiently larger than a_{eff}, the isolated triplet population cannot flow back into the reactive singlet state by spin-state mixing induced by HFI. Consequently, the recombination via the singlet state is inhibited and the radical-pair lifetime is prolonged by the SEMF.

(2) Real-Time Observation of the Spin-State Mixing by a Delay-Shift Experiment. For the detailed and quantitative analysis of the SEMF effect, we have modified the pulse scheme as shown in Figure 5a. The experiment is performed in a static field of 26 mT, and the direction of SEMF is set opposite to the static field. The pulsed field of ΔB, which is identical with or somewhat less than 26 mT, is turned on 150 ns before the laser excitation, which is to say the radical pair is generated in the field of B_{mix} defined as follows:

$$B_{\text{mix}} = 26\text{ mT} - \Delta B \tag{6}$$

The magnetic field that the radical pair experiences is switched from B_{mix} to 26 mT when the pulsed field is turned off. The time interval between the laser pulse and the falling edge of the pulsed field is defined as t_d, which is the delay time of the field switching.

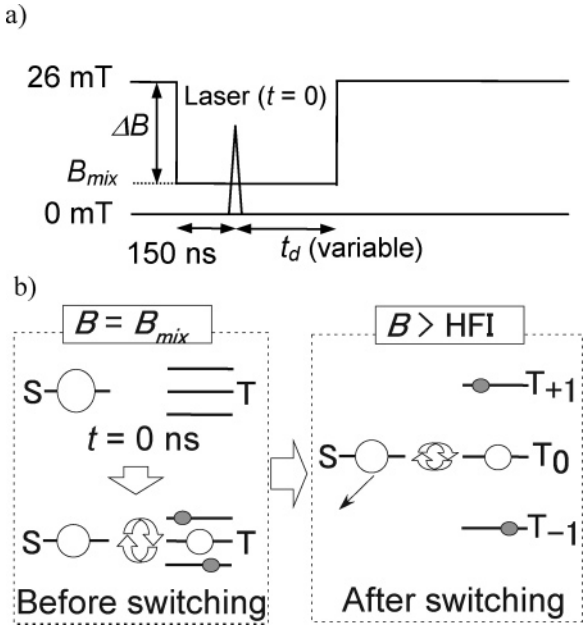

Figure 5. (a) Pulse sequence of SEMF used in the delay-shift experiment. (b) Time evolution of spin states under this pulse sequence.

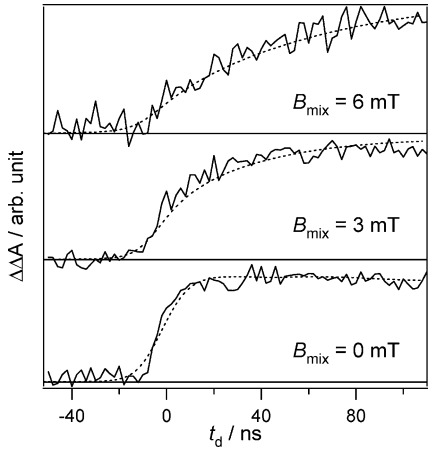

Figure 6. Delay time (t_d) dependence of the SEMF effect obtained as described in Figure 5 for $B_{\text{mix}} = 0$, 3, and 6 mT (solid lines). Broken lines are simulated curves calculated using the modified Liouville equation described in the text.

Here we explain the concept of the real-time observation of the spin-state mixing process using this pulse scheme (Figure 5b). The idea is similar to that of pulsed MARY spectroscopy described in ref 13. Because the photocleavage reaction is quite fast, we can say that the $S-T_{\pm1}$ mixing begins with the laser excitation in the field of B_{mix}. Then, the spin-state mixing is stopped when the field is switched back to 26 mT. The important point here is that the radical pair undergoes the spin-state mixing only in the period t_d in the low magnetic field of B_{mix}. The increment in the radical yield produced by the field switching relative to the yield obtained at static 26 mT directly reflects the radical-pair population developed in the $T_{\pm1}$ states by the spin-state mixing that occurs only during the interval of t_d (colored gray in Figure 5b). Consequently, the t_d dependence of the SEMF effect (delay-shift experiment) at several B_{mix} fields provides the real-time observation of the $S-T_{\pm1}$ spin-state mixing process in weak magnetic fields.

The experimental results of the delay-shift experiment of SEMF are shown in Figure 6. The SEMF effect is evaluated by the subtraction of the transient absorption signal as

$$\Delta\Delta A = \Delta A(\mathrm{SEMF}) - \Delta A(B = 26\ \mathrm{mT}) \quad (7)$$

The time average of the flat component of $\Delta\Delta A$ (1.5−4.5 μs after laser shot), which corresponds to the change in the free-radical yield, is plotted as a function of t_d.

We have successfully observed the $S-T$ mixing of the radical pair at a weak magnetic field for the first time in a photogenerated radical-pair system. However, the fastest rise time of ca. 10 ns observed in the case of $B_{mix} = 0$ mT is thought to be nearly the instrumental function, mainly limited by the duration and/or jitter of the laser pulse. This indicates that the spin-state mixing in 0 mT is comparable to or faster than 10 ns. This time scale is quite reasonable because the characteristic time scale of spin-state mixing induced by the HFI is about 10 ns. Thus, it is difficult to extract information about the dephasing process from the obtained time profile, which is distorted by the laser pulse with a comparable duration to the frequency of the coherent spin-state mixing.

Interestingly, the time profiles in the case of $B_{mix} = 3$ and 6 mT show much slower rising components than that in 0 mT, 18 and 43 ns, respectively. Such a mixing feature has not been observed in the system of short-lived radical pairs generated by radiolysis in homogeneous solutions.[32,33] The spin-state mixing process detected by delayed fluorescence in such systems shows a coherent feature, and the time scale is almost independent of the applied magnetic field. This is due to the short lifetime and the small reencounter probability of the radical pair in such systems, which fully separate the spin dynamics from the diffusive molecular motion. Our result clearly demonstrates the existence of an incoherent spin-state mixing process that is considered to be characteristic of micellized radical pairs, which are so long-lived that the spin dynamics couples to their diffusive motion in the micellar cage.

The observed incoherent mixing with a time scale of a few tens of nanoseconds is considered to be much faster than conventional T_1 relaxation, which is generally longer than 100 ns. Thus, the incoherent mixing is attributed to interplay between coherent spin mixing by HFI and fast dephasing caused by the fluctuation of J and/or D as suggested by time-resolved MARY spectra.

(III) Mechanism of the Incoherent Spin-State Mixing. The effect of dephasing processes on the coherent spin-state mixing is roughly explained by the simple quantum mechanics of two states, for example, $|S\rangle$ and $|T_{+1}\rangle$ extracted from four radical-pair spin states, coupled by a matrix element V (HFI in this case), as shown in refs 13 and 14. An energy gap of these two states is considered to be linearly proportional to the external magnetic field (B_0) as

$$\Delta\omega \sim g\mu_B B_0/\hbar \quad (8)$$

where g and μ_B are the averaged g value of the radical pair and Bohr magneton, respectively. The amplitude of the matrix element is expressed as

$$V = -a_{eff}/2\sqrt{2} \quad (9)$$

In the absence of the dephasing process, one can analytically calculate the time evolution of the population difference as

$$P(t) = [S(t)] - [T_{+1}(t)] = \cos\omega' t + \frac{\Delta\omega^2}{\omega'^2}(1 - \cos\omega' t) \quad (10)$$

where

$$\omega' = \sqrt{4V^2 + \Delta\omega^2} = \sqrt{\frac{a_{eff}^{\ 2}}{2} + \Delta\omega^2} \quad (11)$$

Thus, the time average of the population difference

$$\overline{P(t)} = \frac{\Delta\omega^2}{\frac{a_{eff}^{\ 2}}{2} + \Delta\omega^2} \quad (12)$$

is drastically increased by the applied magnetic field. The so-called hyperfine mechanism is roughly explained as noted above. It should be noted that the frequency ω' does not change significantly or become larger in an applied magnetic field comparable to the HFI. This feature is consistent with the spin-state mixing observed in the radical-pair systems generated by radiolysis.[32,33]

The dephasing process comparable to the spin-state mixing frequency changes the mixing feature depending on the amplitude of the magnetic field. In zero magnetic field, the coherence is damped on the time scale of the dephasing rate (k_{dep}) and reaches $P = 0$ at late time. However, the time scale and time-averaged population difference are almost the same as those without dephasing. That is why we have observed only a fast rising of ca. 10 ns in zero magnetic field.

The situation is completely different when a magnetic field comparable to the HFI is applied. Fast damping of the coherence between two states induces an incoherent spin-state mixing process at later time and finally reaches $P = 0$. Though this feature is apparently indistinguishable from ordinary longitudinal relaxation (T_1), the incoherent population transfer can be induced by interplay between the coherent interaction and the fast dephasing process even without the direct T_1 process. The time scale of incoherent mixing is slower than that of coherent mixing or the dephasing rate itself depending on the applied magnetic field. If the dephasing rate is fast enough compared with the time scale of a_{eff}, the spin-state mixing becomes fully incoherent and the rate of spin-state mixing is obtained as

$$\frac{1}{T_1^{\ eff}} = \frac{k_{dep}a_{eff}^{\ 2}/2}{k_{dep}^{\ 2} + \Delta\omega^2} \quad (13)$$

by an analytical solution of the Broch equation.[13,14] Here we notice that the incoherent mixing becomes slower when the magnetic field B_0 ($\propto\Delta\omega$) is increased. This prediction is seemingly consistent with the experimental result of the B_{mix} dependence of the shift experiment, but the assumption might not be true in this system.

If the dephasing rate, magnetic field, and a_{eff} are all comparable, the spin-state mixing shows a biphasic feature, namely, fast coherent mixing at early time and slow incoherent mixing at later time. Thus, in the case of $B_{mix} = 3$ mT, the obtained time profile might retain the coherent feature at the earliest time, which is followed by the incoherent mixing process. Computational simulations allow us more quantitative analysis.

(IV) Theoretical Simulation of the SEMF Effect. For detailed analysis, we have carried out theoretical simulations as described in the Theory section. The simulated results of the shift experiment of SEMF are shown by broken lines in Figure 6. The experimental curves are reproduced well by the simulation with reasonable parameters. A little deviation at relatively short t_d might be due to the difference between the Gaussian time profile and the real laser pulse. The time profiles obtained

by simulation of SEMF with each B_{mix} qualitatively correspond with the calculated time evolutions of the $T_{\pm1}$ population in the respective fields, convoluted by the laser pulse (Supporting Information). This indicates that we have certainly observed the $S-T_{\pm1}$ mixing in low fields by the SEMF shift experiment.

The simulated time profile in the case of $B_{mix} = 0$ mT is insensitive to the dephasing parameters because of the instrumental function. On the other hand, the simulated time profiles in the case of $B_{mix} = 3$ and 6 mT depend on w_{STD} and w_{TTD}. Particularly, the simulated time profile in the case of 3 mT is quite sensitive to w_{STD} and w_{TTD}, which affect the spin-state mixing feature differently as described later and are determined almost independently to be $w_{STD} = 2 \times 10^8$ s^{-1} and $w_{TTD} = 0.2 \times 10^8$ s^{-1}, respectively. This is the first successful example of the separate determination of two dephasing parameters in low magnetic field.

The parameters for intraradical relaxation, which are τ_c and [*A*:*A*], have little influence on simulated curvature as long as they are in the range of reasonable values; they are set to 30 ps and 5 mT^2, respectively.[13,14] This fact indicates that the spin dynamics are governed by the cooperative action of dephasing and HFI in magnetic fields comparable to the HFI. Obtained total dephasing rates are reasonable for micellized radical pairs because their reencounter frequency is said to be $\sim 10^8$ s^{-1}.[34,35]

The effect of STD and TTD on the simulated time profile at $B_{mix} = 3$ mT differs to some extent, whereas their effect on the low-field spin dynamics is identical in triplet radical-pair systems.[4,13,14] The reason is explained as follows; in the case of a singlet-born radical pair, only $S-T$ mixing works at the earliest times because the initial state is a pure singlet state. $S-T$ mixing is followed by populating triplet states and quantum-mechanical interference with $T-T$ mixing. Thus, STD can affect spin mixing at earlier times than TTD does. For this reason, faster STD can quench the first coherent cycle of the spin-state mixing more effectively, resulting in a faster rise of the incoherent mixing process, which smoothly follows the first half-cycle of the coherent mixing (Supporting Information). On the other hand, TTD cannot affect the first coherent cycle, and it remains almost the same as that without any dephasing process. In order to fit both the fast rise at early time and the saturating feature at later time of the experimental time profile, the fast STD rate of 10^8 s^{-1} is needed. In this case, a slow TTD rate of 10^7 gives better fitting results than those without a TTD process.

The difference in the obtained STD and TTD rate constants is considered to reflect the efficiency of *J* and *D* as sources of these dephasing processes. *J* causes an energy gap between the singlet and triplet spin states but does not affect the energy splitting within three triplet sublevels. Fluctuation of *J* by a reencounter process thus induces only STD. On the other hand, *D* affects both singlet−triplet and triplet−triplet energy gaps. Furthermore, *D* is dependent on both the inter-radical distance and angle between the magnetic field and the principal axes of the radical pair. Thus, the effect of *D* is more complicated than that of *J*; namely, fluctuation of *D* by reencounter and/or diffusion causes both STD and TTD. Simply stated, STD is likely to be faster than TTD because the two dephasing sources work together.

The STD rate constant obtained by our SEMF experiment is 10 times faster than that obtained by time-resolved X-band EPR spectroscopy in this system.[25] The cause of this deviation is still unclear; however, it is likely due to the difference in the field strength and/or dephasing states. In the case of the transient EPR observed in the field of 330 mT, the effect of the STD mainly appears as the population relaxation between the middle two states, which are referred to as $S-T_0$ mixed states, of the SCRP.[36] In this case, one can selectively observe a $S-T_0$ dephasing process by the time dependence of the SCRP phase pattern.

In the present case, we can selectively observe the $S-T_{\pm1}$ mixing at weak magnetic fields by means of SEMF, which is assumed to be the transient projection of the $T_{\pm1}$ character of the radical pair. The obtained STD rate is understood as a rate of dephasing between singlet and $T_{\pm1}$ states, which are coherently mixing by the HFI.

The simulation carried out here seems to show the limitation of the modified single-site model for quantitative analysis of the dynamics of long-lived radical pairs. A trial of Monte Carlo simulation,[37] in which the fluctuation of *J* and *D* by molecular diffusion is directly taken into account, is underway. Nonetheless, the real-time observation of the $S-T$ mixing process by means of the SEMF experiment is a powerful tool for detecting the spin dynamics of long-lived radical pairs in low magnetic fields. Especially in the singlet-born system, the time profile obtained is quite sensitive to the dephasing parameters, which reflect inter-radical interactions and their fluctuation by molecular diffusion dynamics in confined conditions.

In conclusion, we have observed the singlet−triplet spin-state mixing process of the singlet-born micellized radical pair by means of a delay-shift experiment of nanosecond SEMF. The observed incoherent mixing process in low magnetic field is explained by interplay between coherent HFI and fast dephasing processes characteristic of micellar systems. Our results demonstrate the potentiality of low-field spin dynamics as a probe of the molecular dynamics of long-lived radical pairs confined in inhomogeneous environments including biological reaction systems.

Acknowledgment. We thank Dr. Kiminori Maeda, Dr. Jonathan R. Woodward, and Dr. Yasuhiro Kobori for their stimulating discussion. This work is financially supported by a Grant-in-Aid for JSPS Fellows (No. 1806998).

Supporting Information Available: Dependence of simulated time evolution of the $T_{\pm1}$ population on STD and TTD rate constants. This material is available of free of charge via the Internet at http://pubs.acs.org.

References and Notes

(1) Steiner, U. E.; Ulrich, T. *Chem. Rev.* **1989**, *89*, 51.
(2) Brocklehurst, B.; McLauchlan, K. A. *Int. J. Radiat. Biol.* **1996**, *69*, 3.
(3) Eveson, R. W.; Timmel, C. R.; Brocklehurst, B.; Hore, P. J.; McLauchlan, K. A. *Int. J. Radiat. Biol.* **2000**, *76*, 1509.
(4) Suzuki, T.; Miura, T.; Maeda, K.; Arai, T. *J. Phys. Chem. A* **2006**, *110*, 4151.
(5) Ritz, T.; Adem, S.; Schulten, K. *Biophys. J.* **2000**, *78*, 707.
(6) Ritz, T.; Thalau, P.; Phillips, J. B.; Wiltschko, R.; Wiltschko, W. *Nature* **2004**, *429*, 177.
(7) Giovani, B.; Byrdin, M.; Ahmad, M.; Brettel, K. *Nat. Struct. Biol.* **2003**, *10*, 489.
(8) Liedvogel, M.; Maeda, K.; Henbest, K.; Schleicher, E.; Simon, T.; Timmel, C. R.; Hore, P. J.; Mouritsen, H. *PLoS one* **2007**, e1106.
(9) Miura, T.; Maeda, K.; Arai, T. *J. Phys. Chem. B* **2003**, *107*, 6474.
(10) Kobori, Y.; Norris, J. R. *J. Am. Chem. Soc.* **2006**, *128*, 4.
(11) Stass, D. V.; Lukzen, N. N.; Tadjikov, B. M.; Molin, Y. N. *Chem. Phys. Lett.* **1995**, *233*, 444.
(12) Batchelor, S. N.; Kay, C. W.; McLauchlan, K. A.; Shkrob, I. A. *J. Phys. Chem.* **1993**, *97*, 13250.
(13) Miura, T.; Maeda, K.; Arai, T. *J. Phys. Chem. A* **2006**, *110*, 4151.
(14) Maeda, K.; Miura, T.; Arai, T. *Mol. Phys.* **2006**, *104*, 1779.
(15) Shushin, A. I. *Chem. Phys. Lett.* **1994**, *181*, 274.
(16) Tadjikov, B. M.; Astashkin, A. V.; Sakaguchi, Y. *Chem. Phys. Lett.* **1998**, *283*, 179.

(17) Gorelik, V. R.; Maeda, K.; Yashiro, H.; Murai, H. *J. Phys. Chem*. **2001**, *105*, 8011.
(18) Gattermann, L.; Wieland, T. *Die Praxis des Organischen Chimikers*; De Gruyter: Berlin, 1958.
(19) Kageyama, A.; Yashiro, H.; Murai, H. *Mol. Phys*. **2002**, *100*, 1341.
(20) Sloop, D. J.; Lin, T.; Ackerman, J. J. H. *J. Magn. Reson*. **1999**, *139*, 60.
(21) Schulten, K.; Wolynes, P. G. *J. Chem. Phys*. **1978**, *68*, 3292.
(22) Lenderink, E.; Duppen, K.; Wiersma, D. A. *Chem. Phys. Lett*. **1992**, *194*, 403.
(23) Carrington, A.; McLachlan, A. D. *Introduction to Magnetic Resonance with Applications to Chemistry and Chemical Physics*; Harper & Row: New York, 1967.
(24) Fukuju, T.; Yashiro, H.; Maeda, K.; Murai, H.; Azumi, T. *J. Phys. Chem. A* **1997**, *101*, 7783.
(25) Fukuju, T.; Yashiro, H.; Maeda, K.; Murai, H. *Chem. Phys. Lett.* **1999**, *304*, 173.
(26) Sakaguchi, Y.; Hayashi, H. *J. Phys. Chem*. **1984**, *88*, 1437.
(27) DiLabio, G. A.; Litwinienko, G.; Lin, S.; Pratt, D. A.; Ingold, K. U. *J. Phys. Chem. A* **2002**, *106*, 11719.
(28) Hayashi, H.; Nagakura, S. *Bull. Chem. Soc. Jpn*. **1984**, *57*, 322.
(29) Okazaki, M.; Tai, Y.; Nunome, K.; Toriyama, K.; Nagakura, S. *Chem. Phys*. **1992**, *161*, 177.
(30) Neugebauer, F. A.; Bamberger, S. *Chem. Ber*. **1974**, *107*, 2362.
(31) Rodgers, C. T.; Norman, S. A.; Henbest, K. B.; Timmel, C. R.; Hore, P. J. *J. Am. Chem. Soc.* **2007**, *129*, 6746.
(32) Salikhov, K. M.; Molin, Y. N.; Sagdeev, R. Z.; Buchachenko, A. L. *Spin Polarization and Magnetic Effects in Radical Reactions*; Elsevier: Amsterdam, The Netherlands, 1984.
(33) Bagryansky, V. A.; Usov, O. M.; Borovkov, V. I.; Kobzeva, T. V.; Molin, Y. N. *Chem. Phys.* **2000**, *255*, 237.
(34) Tarasov, V. F.; Bagranskaya, E. G.; Shkrob, I. A.; Avdievich, N. I.; Ghatlia, N. D.; Lukzen, N. N.; Turro, N. J.; Sagdeev, R. Z. *J. Am. Chem. Soc*. **1995**, *117*, 110.
(35) Tarasov, V. F.; Yashiro, H.; Maeda, K.; Azumi, T.; Shkrob, I. A. *Chem. Phys.***1996**, *212*, 353.
(36) Terazima, M.; Maeda, K.; Azumi, T.; Tanimoto, Y. *Chem. Phys. Lett.* **1989**, *164*, 562.
(37) O'Dea, A. R.; Curtis, A. F.; Green, N. J. B.; Timmel, C. R.; Hore, P. J. *J. Phys. Chem. A* **2005**, *109*, 869.